

Oxygen Transport Ceramic Membranes

Quarterly Report

January 2006 – March 2006

Principal Authors:

Prof. S. Bandopadhyay

Dr. T. Nithyanantham

Issued: May 2006

DOE Award # DE-FC26-99FT40054

**University of Alaska Fairbanks
Fairbanks, AK 99775**

Contributing Authors:

1. **X.-D Zhou, Y-W. Sin and H. U. Anderson**, Materials Research Center, University of Missouri-Rolla, Rolla, MO 65401
2. **Prof. Alan Jacobson and Prof. C.A. Mims**; University of Houston/University of Toronto

DISCLAIMER

This report was prepared as an account of the work sponsored by an agency of the United States Government. Neither the United States Government nor any agency thereof, nor any of their employees, makes any warranty, express or implied, or assumes any legal liability or responsibility for the accuracy, completeness, or usefulness of any information, apparatus, product, or process disclosed, or represents that its use would not infringe privately owned rights. Reference herein to any specific commercial product, process, or service by trade name, trademark, manufacturer, or otherwise does not necessarily constitute or imply its endorsement, recommendation, or favoring by the United States Government or any agency thereof. The views and opinions of authors expressed herein do not necessarily state or reflect those of the United States Government or any agency thereof.

ABSTRACT

In this quarter a systematic analysis on the decomposition behavior of the OTM membranes at air and nitrogen were initiated to understand the structural and stoichiometric changes associated with elevated temperatures. Evaluation of the flexural strengths using 4-point bend test was also started for the dual phase membranes. Initial results on the synthesis of dual phase composite materials have been obtained. The measurements have focused on the compatibility of mixed conductors with the pure ionic conductors yttria stabilized zirconia (YSZ) and gadolinium doped ceria (GDC). The initial results obtained for three different mixed conductors suggest that (GDC) is the better choice. A new membrane permeation system has been designed and tested and sintering studies of biphasic systems are in progress.

TABLE OF CONTENTS

| | |
|---|----|
| INTRODUCTION | 1 |
| EXECUTIVE SUMMARY | 3 |
| • Determine material mechanical properties under conditions of high temperature and reactive atmosphere | 4 |
| • Measurement of Surface Activation/Reaction rates in Ion Transport Membranes using Isotope Tracer and Transient Kinetic Techniques | 13 |
| CONCLUSIONS | 21 |
| LISTS OF ACRONYMS AND ABBREVIATIONS | 22 |
| REFERENCES | 23 |

LIST OF GRAPHICAL MATERIALS

- Figure 1. (a). Change in weight (b) DTA and temperature data as function of time for LSFT in air and N₂ environment
- Figure 2. (a) Change in weight (b) DTA and temperature data as function of time for LSFT-CGO in air and N₂ environment.
- Figure 3. LSFT-CGO specimen on the 4-point fixture (a) before (b) after strength test at room temperature.
- Figure 4. Stereo micrographs of fracture surfaces of LSFT-CGO after strength tests (a) at room temperature and (b) at 1000°C in N₂
- Figure 5. Load-Displacement plots for dual phase membranes.
- Figure 6. Strength-Displacement plots for dual phase membranes.
- Figure 7. The structures of La_{0.7}Sr_{0.3}Cu_{0.2}Fe_{0.8}O_{3-δ}, La₂NiO_{4+x} and PrBaCo₂O_{5+x}
- Figure 8. X-ray diffraction patterns of the reaction for (a) 50/50 wt. % 8-YSZ/La_{0.7}Sr_{0.3}Cu_{0.2}Fe_{0.8}O_{3-δ} at $850 \leq T \leq 1000$ °C (b) expanded in the range $25 \leq 2\theta \leq 45^\circ$.
- Figure 9. X-ray data showing the absence of reaction between PrBaCo₂O₅ and CeO₂.
- Figure 10 Thermal and chemical expansion of PrBaCo₂O₅ (PBCO) and NdBaCo₂O₅ (NBCO).

LIST OF TABLES

- Table 1. Change in weight and corresponding temperatures of OTM membranes in air and N₂ environment

INTRODUCTION

Conversion of natural gas to liquid fuels and chemicals is a major goal for the Nation as it enters the 21st Century. Technically robust and economically viable processes are needed to capture the value of the vast reserves of natural gas on Alaska's North Slope, and wean the Nation from dependence on foreign petroleum sources. Technologies that are emerging to fulfill this need are all based syngas as an intermediate. Syngas (a mixture of hydrogen and carbon monoxide) is a fundamental building block from which chemicals and fuels can be derived. Lower cost syngas translates directly into more cost-competitive fuels and chemicals.

The currently practiced commercial technology for making syngas is either steam methane reforming (SMR) or a two-step process involving cryogenic oxygen separation followed by natural gas partial oxidation (POX). These high-energy, capital-intensive processes do not always produce syngas at a cost that makes its derivatives competitive with current petroleum-based fuels and chemicals.

In the mid 80's BP invented a radically new technology concept that will have a major economic and energy efficiency impact on the conversion of natural gas to liquid fuels, hydrogen, and chemicals.¹ This technology, called Electropox, integrates oxygen separation with the oxidation and steam reforming of natural gas into a single process to produce syngas with an economic advantage of 30 to 50 percent over conventional technologies.²

The Electropox process uses novel and proprietary solid metal oxide ceramic oxygen transport membranes [OTMs], which selectively conduct both oxide ions and electrons through their lattice structure at elevated temperatures.³ Under the influence of an oxygen partial pressure gradient, oxygen ions move through the dense, nonporous membrane lattice at high rates with 100 percent selectivity. Transported oxygen reacts with natural gas on the fuel side of the ceramic membrane in the presence of a catalyst to produce syngas.

¹Mazanec, T. J.; Cable, T. L.; Frye, J. G., Jr.; US 4,793,904, 27 Dec **1988**, assigned to The Standard Oil Company (now BP America), Mazanec, T. J.; Cable, T. L.; US 4,802,958, 7 Feb **1989**, assigned to the Standard Oil Co. (now BP America), Cable, T. L.; Mazanec, T. J.; Frye, J. G., Jr.; European Patent Application 0399833, 24 May **1990**, published 28 November **1990**.

²Bredesen, R.; Sogge, J.; "A Technical and Economic Assessment of Membrane Reactors for Hydrogen and Syngas Production" presented at Seminar on the Ecol. Applic. of Innovative Membrane Technology in the Chemical Industry", Cetraro, Calabria, Italy, 1-4 May **1996**.

³Mazanec, T.J., *Interface*, **1996**; Mazanec, T.J., *Solid State Ionics*, 70/71, **1994** 11-19; "Electropox: BP's Novel Oxidation Technology", T.J. Mazanec, pp 212-225, in "The Role of Oxygen in Improving Chemical Processes", M. Fetizon and W.J. Thomas, eds, Royal Society of Chemistry, London, **1993**; "Electropox: BP's Novel Oxidation Technology", T.J. Mazanec, pp 85-96, in "The Activation of Dioxygen and Homogeneous Catalytic Oxidation", D.H.R. Barton, A. E. Martell, D.T. Sawyer, eds, Plenum Press, New York, **1993**; "Electrocatalytic Cells for Chemical Reaction", T.J. Mazanec, T.L. Cable, J.G. Frye, Jr.; Prep Petrol Div ACS, San Fran, **1992** 37, 135-146; T.J. Mazanec, T.L. Cable, J.G. Frye, Jr.; *Solid State Ionics*, **1992**, 53-56, 111-118.

In 1997 BP entered into an OTM Alliance with Praxair, Amoco, Statoil and Sasol to advance the Electropox technology in an industrially sponsored development program. These five companies have been joined by Phillips Petroleum and now are carrying out a multi-year \$40+ million program to develop and commercialize the technology. The program targets materials, manufacturing and engineering development issues and culminates in the operation of semi-works and demonstration scale prototype units.

The Electropox process represents a truly revolutionary technology for conversion of natural gas to synthesis gas not only because it combines the three separate unit operations of oxygen separation, methane oxidation and methane steam reforming into a single step, but also because it employs a chemically active ceramic material in a fundamentally new way. On numerous fronts the commercialization of Electropox demands solutions to problems that have never before been accomplished. Basic problems in materials and catalysts, membrane fabrication, model development, and reactor engineering all need solutions to achieve commercial success. Six important issues have been selected as needing understanding on a fundamental level at which the applied Alliance program cannot achieve the breadth and depth of understanding needed for rapid advancement. These issues include:

1. Oxygen diffusion kinetics (University of Houston);
2. Phase stability and stress development (University of Missouri - Rolla);
3. Mechanical property evaluation in thermal and chemical stress fields (University of Alaska Fairbanks)

Statement of Work

Task 1 Evaluate phase stability and thermal expansion of candidate perovskite membranes and develop techniques to support these materials on porous metal structures.

Task 2 Determine materials mechanical properties under conditions of high temperatures and reactive atmospheres.

Task 3 Measure kinetics of oxygen uptake and transport in ceramic membrane materials under commercially relevant conditions using isotope labeling techniques.

EXECUTIVE SUMMARY

Research on the Oxygen Transport Membranes is being performed at the various universities under the stewardship of Praxair. This quarterly technical report presents the progress of the tasks defined to understand the fundamental concepts and structural performance of the OTM material.

LSFT and LSFT-CGO membranes exhibit a reversible weight loss along with the irreversible weight loss when they are heated in air. The reversible weight loss is mainly due to the loss of oxygen at high temperature. The total weight loss in the N₂ atmosphere is significantly higher than the weight loss occurred in air. The flow of N₂ has caused more oxygen desorption. Also, the weight loss is completely irreversible in N₂ atmosphere. Overall, in N₂ atmosphere, the decomposition of membranes starts earlier than it was observed in air.

Evaluation of flexural strength at room temperature and at 1000°C in N₂ atmosphere was carried out for LSFT-CGO membrane. The flexural strength value obtained for dual phase membrane (LSFT-CGO) at room temperature and at 1000°C in N₂ is 245 and 107.5 MPa respectively.

The thermodynamic properties (stability and phase-separation behavior) and total conductivity of prototype membrane materials will continue to be investigated. These information are needed together with the kinetic information to develop a complete model for the membrane transport. We have previously reported characterization, stoichiometry, conductivity, and dilatometry measurements for several perovskite compositions. In this period, initial results on the synthesis of dual phase composite materials have been obtained. The measurements have focused on the compatibility of mixed conductors with the pure ionic conductors yttria stabilized zirconia (YSZ) and gadolinium doped ceria (GDC). The initial results obtained for three different mixed conductors suggest that (GDC) is the better choice.

**Determine material mechanical properties under conditions of high temperature
and reactive atmosphere**

**Prof. S. Bandopadhyay and Dr. T. Nithyanantham
University of Alaska Fairbanks, AK 99775**

Experimental:

Thermal analysis:

The as-received LSFT and dual phase membranes were cut into small pieces and the thermal analysis were carried out in the air and in the N₂ atmosphere with the heating rate of 20°C/min. The change in weight and endothermic and exothermic process corresponding to different oxygen desorption and structural changes were examined.

Flexural strength:

Test specimens of dimensions (3x4x48 mm) were cut from the bulk, as-sintered bars provided by Praxair. As discussed in previous reports (OTM, Annual Report 2005, Task 2) the tests were done in-situ in a autoclave mounted on a servo-electric loading frame. Loading was done in an in-house designed 4-point flexure with an outer span of 38.1 mm and inner span of 19.05 mm (ASTM-B). The experiments were carried out in room temperature and at 1000°C in inert (N₂) atmosphere. The specimens were polished in all 4 sides and the tensile side was polished using diamond paste of 1 µm prior to the test. The edges of the specimens were also trimmed. In the inert atmosphere, the specimen was loaded in the fixture and heated to 1000°C for 1 hr prior to application of any load. The furnace power was completely shut off after the fracture of the specimen and allowed to cool. A typical flexural strength test usually have a heating period of 2 hrs, dwelling of 1 hr, loading rate as specified and a cool down period of 1000-700°C in 60 min and a 700-200°C in 2 hrs for a sum total of 6-7 hrs.

Results and Discussions:

Thermal analysis:

Figure 1 shows the change in weight, DTA and temperature data as a function of time for LSFT in air and N₂ environment. The temperature and corresponding weight changes are tabulated in Table 1.

Table 1. Change in weight and corresponding temperatures of OTM membranes in air and N₂ environment

| | LSFT | | | | LSFT-CGO | | | |
|---------|------------------|----------------|---------------|----------------|------------------|----------------|---------------|----------------|
| | Temperature (°C) | | Wt Change (%) | | Temperature (°C) | | Wt Change (%) | |
| Heating | Air | N ₂ | Air | N ₂ | Air | N ₂ | Air | N ₂ |
| | 233 | 233 | 0.02 | 0.01 | 211 | 239 | 0.01 | -0.02 |
| | 612 | 523 | 0.03 | 0.02 | 515 | | 0.02 | |
| | 723 | 624 | 0.0 | 0.0 | | | | |
| | 1000 | 1000 | -0.62 | -0.93 | 1000 | 1000 | -0.23 | -0.51 |
| Cooling | 575 | 452 | -0.33 | -0.95 | 500 | 500 | -0.07 | -0.58 |
| | 100 | 100 | -0.35 | -0.97 | 100 | 100 | -0.09 | -0.6 |

With increasing temperature, the samples exposed in air gained a marginal weight before a major weight loss starting from 723°C. A maximum weight loss 0.62% was observed during the heating of the sample at 1000°C. There was no significant weight loss during dwelling at 1000°C in air. A significant amount of this weight loss is reversible mainly due to the absorption of oxygen. This is reflected by the weight gain (Figure 1a). The reversible weight loss is observed till the temperature reaches 575°C during cooling. The exothermic and endothermic reactions are shown in Figure 1b.

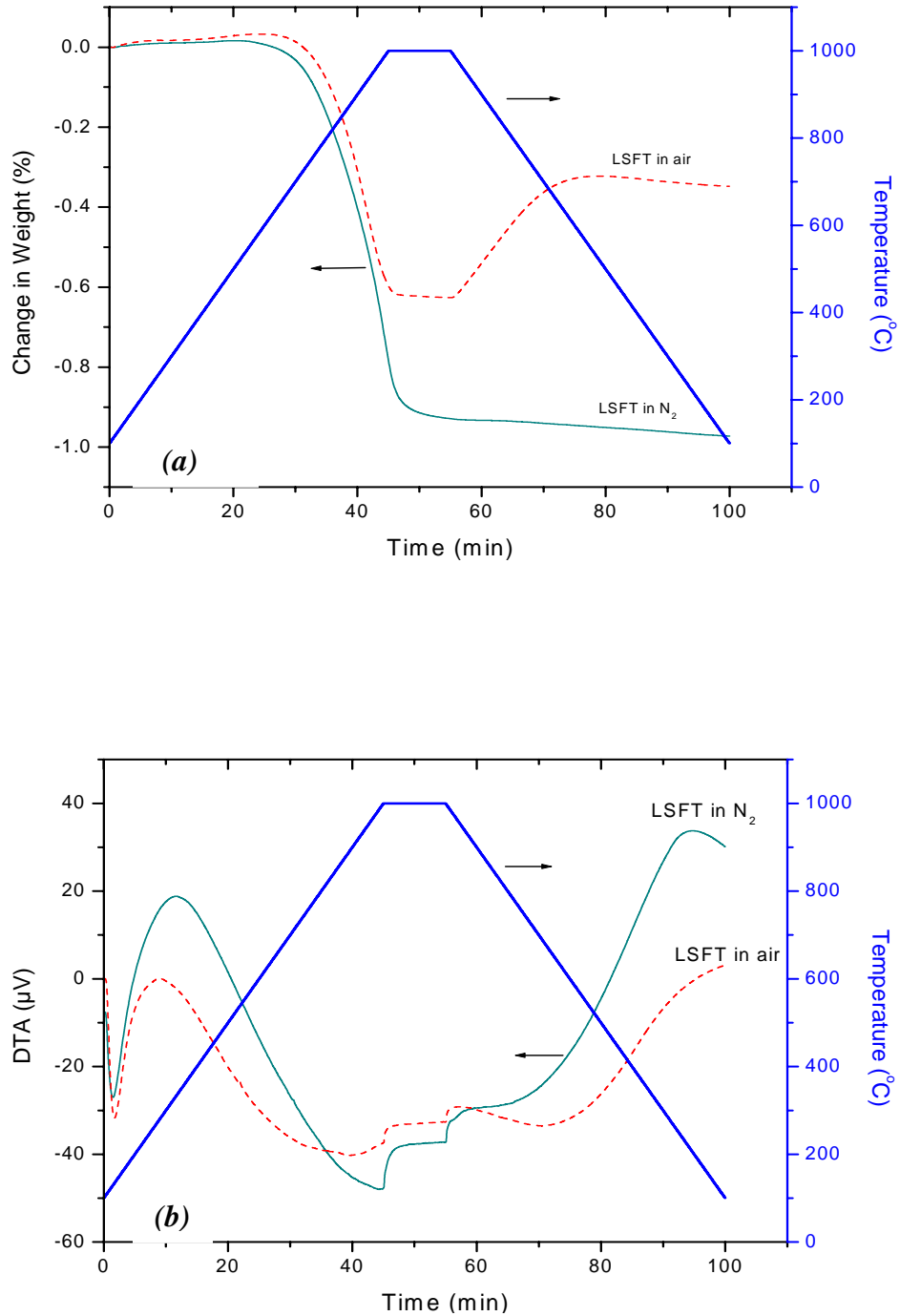


Figure 1 (a). Change in weight (b) DTA and temperature data as function of time for LSFT in air and N₂ environment

The reversible weight loss of 0.29% is observed for LSFT in air which is slightly lesser than the weight loss value obtained for annealed LSFT in air as reported by Zhou *et*

al^1 , the value of which was 0.65%. An irreversible weight loss of 0.33% was observed during the present analysis. This irreversible weight loss may be due to the volatile organic substances. Calcination of the membrane at 1200°C can be helpful in minimizing the irreversible weight loss, caused by the volatile species.

The total weight loss in the N₂ atmosphere is significantly higher than the weight loss occurred in air. The maximum weight loss at 1000°C in N₂ is 0.93%. The flow of N₂ has caused more oxygen desorption. Also absorption of oxygen during cooling was not possible. This has resulted a continuous weight loss even during cooling after dwelling at 1000°C, even though the rate of weight loss has decreased significantly during cooling cycle. The major weight loss has started 100°C earlier during heating with the flow of N₂. This behavior has raised questions about the early decomposition products which may need to be studied in detail.

The change in weight with the function of time in the LSFT-CGO membrane in air and N₂ environment is shown in Figure 2. In air a maximum weight loss of 0.23% was observed at the maximum temperature, 1000°C. Prior to this significant weight change, two small events of weight gains were observed. There is no noticeable weight loss after the temperature has reached the steady state during dwelling. The cooling has resulted in the positive weight change which lasts till 500°C. The reversible weight loss was about 0.07% and the remaining weight loss caused during heating can be considered as irreversible. The higher percentage (69.56%) of reversible weight loss observed for dual phase membrane suggests the presence of volatile substances in the dual phase membrane and comparatively lesser than the LSFT.

In the nitrogen atmosphere the major weight change during heating has started earlier than in air and the total weight loss also higher (0.58%) for the dual phase membrane. There was no reversible weight change with flowing N₂ and the weight loss is continuous even in the cooling cycle as reported for LSFT.

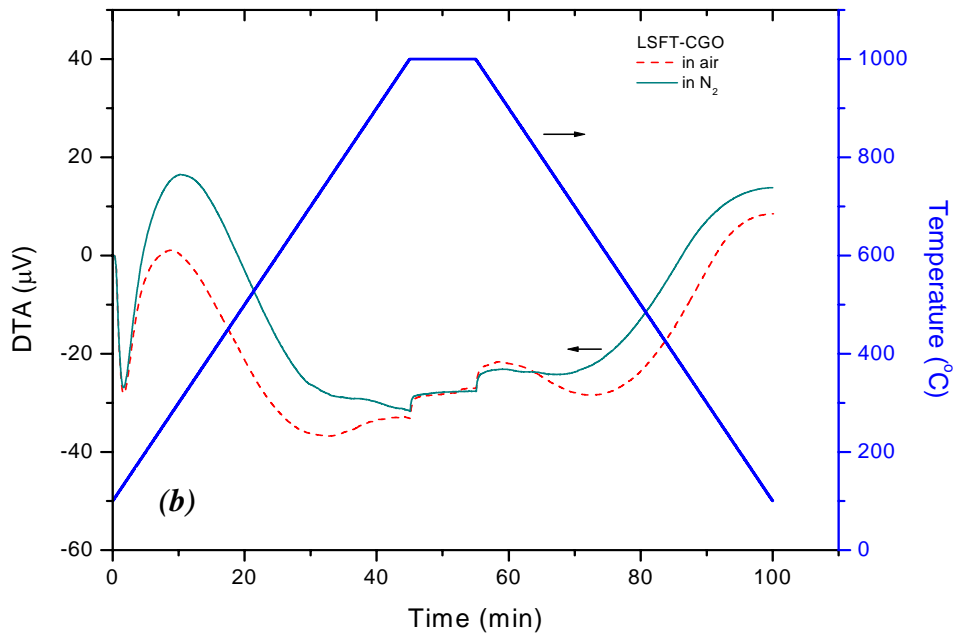
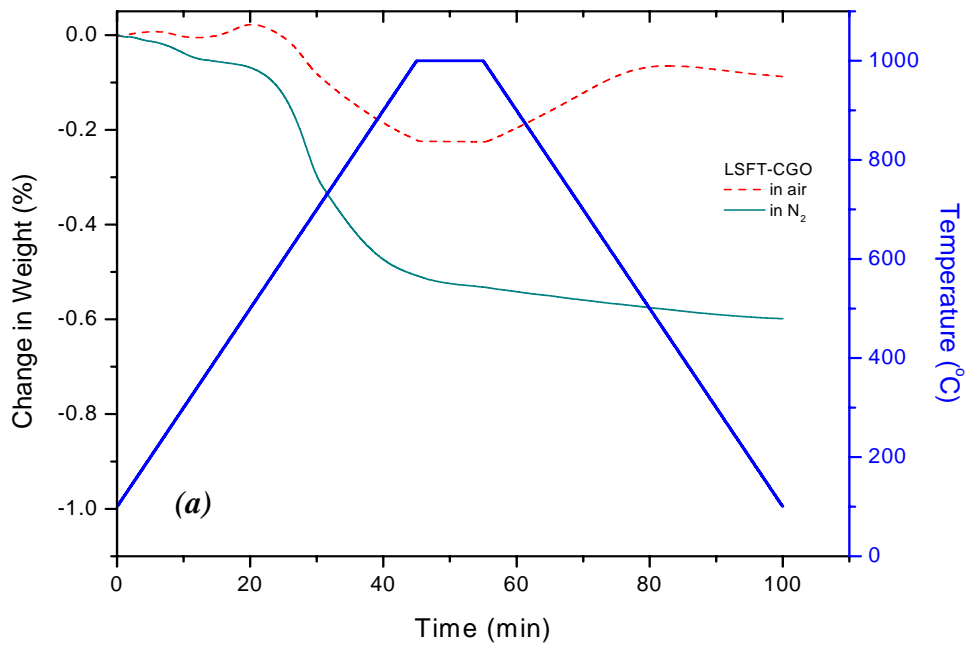


Figure 2. (a) Change in weight (b) DTA and temperature data as function of time for LSFT-CGO in air and N₂ environment.

In general, the weight loss during heating (in both environments) is higher for LSFT than the dual phase membrane and the reversible weight change during cooling is higher for the dual phase membrane.

Flexural strength:

Figure 3 shows the LSFT-CGO specimen on the 4-point fixture before and after strength test at room temperature.

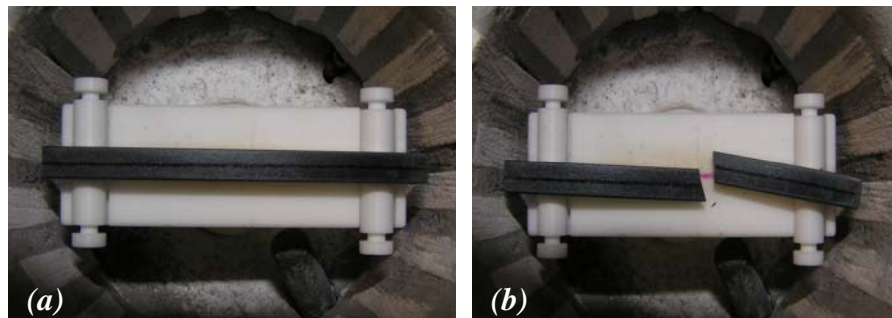


Figure 3. LSFT-CGO specimen on the 4-point fixture (a) before (b) after strength test at room temperature

In room temperature, the dual phase membrane has a flexural strength of 245 MPa and the complete fracture surface is shown in Figure 4(a).

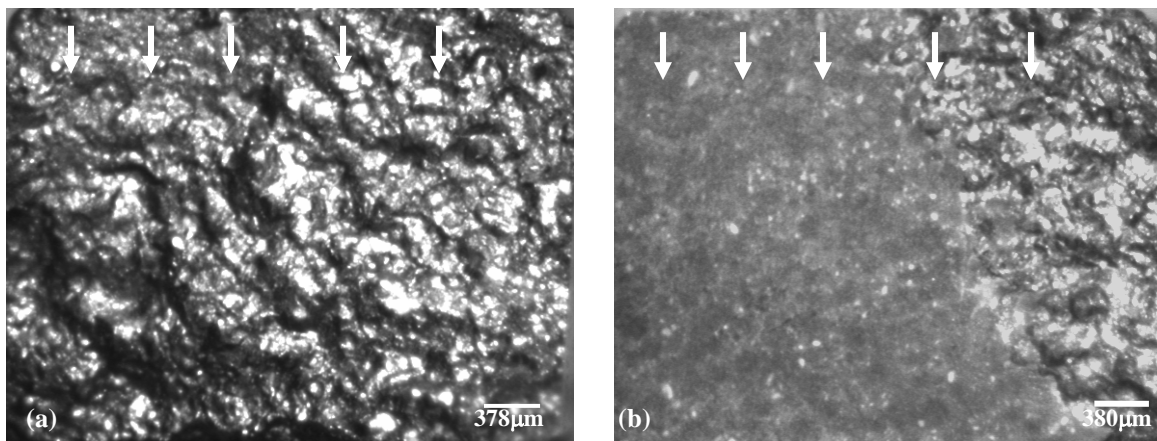


Figure 4. Stereo micrographs of fracture surfaces of LSFT-CGO after strength tests (a) at room temperature and (b) at 1000°C in N₂

The arrow marks show the direction of compressive forces, during loading. The fracture mode appears to be intergranular and the fracture surface (Figure 4a) did not show presence of any volume flaw associated with the fracture. A loading rate of $60\mu\text{m}/\text{min}$ was maintained for both tests. The load-displacement and the strength – displacement plots for the specimen fractured at 1000°C in N_2 environment are also shown in Figure 5 and 6. At 1000°C , in N_2 atmosphere, the dual phase membrane exhibit a flexural strength of 107.5Mpa , which is almost half of the strength it exhibits in the room temperature. Since, the flexural strength of the material is a microstructure sensitive property, the microstructure and presence of flaws can be attributed to the strength of the materials. Hence, the reduction of strength at 1000°C in N_2 environment is related to the microstructural changes occurred to membrane at the elevated temperatures in a reduced atmosphere.

Figure 4(b) shows the change in the fracture morphology in the specimen fractured at 1000°C in N_2 atmosphere. The presence of volume flaw originating from the tensile surface may have caused the fracture during loading. The direction of compressive forces acting upon the specimen is shown by the arrow marks. A detailed SEM analysis on fracture surfaces is needs to be done to understand the fracture behavior.

Figure 5 and 6 also show the change in the slope in the load-displacement plot for the OTM specimen fractured at 1000°C in N_2 atmosphere. The steep slope of the specimen fractured at elevated temperature in reducing environment suggests a change in the binding energy or change in the modulus of elasticity due to the temperature and the environment. These structural properties has to be analysed using X-ray diffraction and thermal analysis.

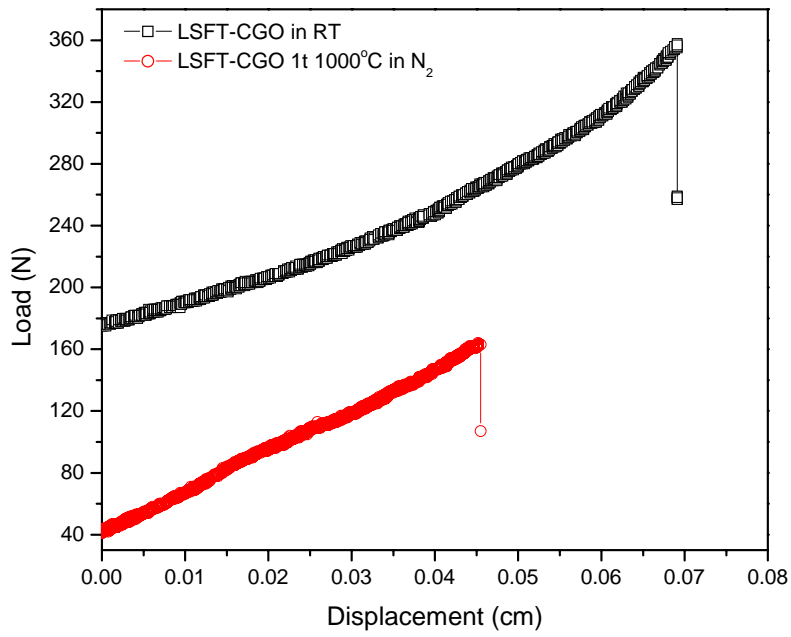


Figure 5. Load-Displacement plots for dual phase membranes.

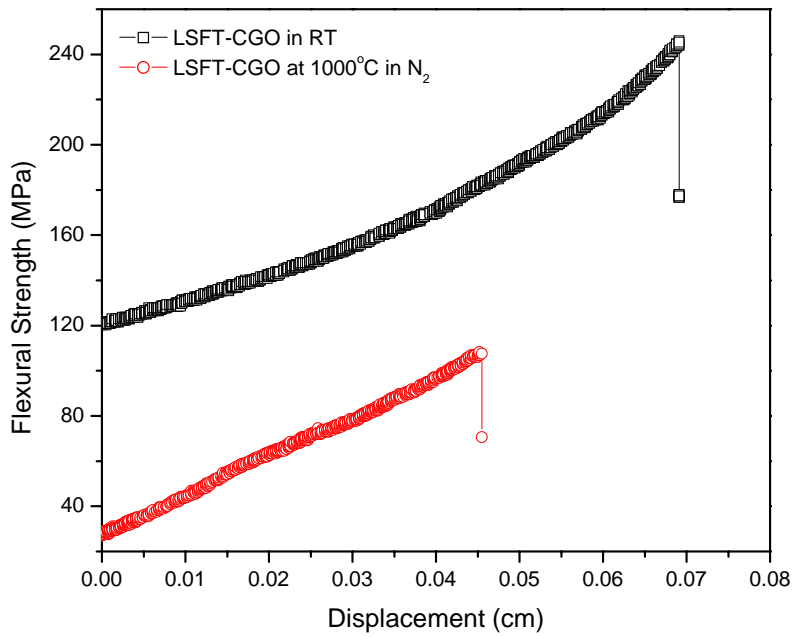


Figure 6. Strength-Displacement plots for dual phase membranes.

Plans for the next quarter:

1. Thermal analysis for calcined OTM specimens and fractured bars will be carried out.
2. SEM analysis of the fractured OTM bars will be carried out to understand the fracture behavior.
3. Systematic analysis of flexural strength in different temperatures with varying strain rates at different atmospheres (air, N₂ and CO₂-CO mixture) will be carried out.

Measurement of Surface Activation/Reaction Rates in Ion Transport Membranes using Isotope Tracer and Transient Kinetic Techniques

A. J. Jacobson, University of Houston, C.A. Mims, University of Toronto

INTRODUCTION

Mixed ionic electronic conductors (MIECs) with the ABO_3 perovskite or related structures have been widely studied because of their practical applications in ion-transport membranes, pressure-driven oxygen generators, partial oxidation reactors, and as electrodes for solid oxide fuel cells (SOFCs) [i]. A number of materials problems remain outstanding for the application of ion transport membrane reactors in the high oxygen partial pressure gradients found, for example, in *syn gas* generation by partial oxidation of methane. The membrane composition must simultaneously provide the necessary oxygen flux and have stability over a wide pO_2 range and appropriate mechanical properties.

The $La_{1-x}Sr_xFeO_{3-x}$ (LSFO) series has high mixed conductivity and better stability than the $La_{1-x}Sr_xCoO_{3-x}$ (LSCO) series but still exhibits limited stability in low- pO_2 environments. Additional substitution on the B-site by metal ions that are more difficult to reduce solves some of these problems but issues remain concerning both kinetic and thermodynamic stability and the effects of composition changes that result from partial decomposition or surface segregation on the membrane surface catalytic properties.

In our studies of membrane materials, we have investigated the pO_2 and temperature dependence of the conductivity, non-stoichiometry and thermal-expansion behavior of two specific compositions, $La_{0.2}Sr_{0.8}Fe_{0.8}Cr_{0.2}O_{3-x}$ and $La_{0.2}Sr_{0.8}Fe_{0.55}Ti_{0.45}O_{3-x}$, by using electrochemical cells and dilatometry [ii iii iv v]. Additional measurements on the simpler composition, $La_{0.5}Sr_{0.5}FeO_{3-x}$ have been made for comparison [vi]. These and other recent studies of ferrites with the perovskite structure show anomalous behavior at low oxygen partial pressures ($<10^{-5}$ atm).

The use of composite membranes offers some potential advantages over single phase materials with respect to improved thermal expansion and mechanical properties. The use

of metal – ionic conductor composites has been reported by a number of authors. The disadvantage of such systems is that the permeation flux is limited by the surface reaction at the three phase boundary between gas, metal and ionic conductor and consequently is much smaller than predicted by an ambipolar diffusion model[vii]. An alternative approach is to combine a mixed electronic ionic conductor with an ionic conductor where the ionic conductor has itself some activity for oxygen reduction. In this quarter we have obtained results on the stability of several examples of this type and obtained enough information to select two systems for further study.

EXPERIMENTAL

We have investigated three types of mixed conductors for potential application in dual phase composites namely a perovskite oxides containing iron and copper ($\text{La}_{0.7}\text{Sr}_{0.3}\text{Cu}_{0.2}\text{Fe}_{0.8}\text{O}_{3-\delta}$) $\text{La}_2\text{NiO}_{4+x}$ and the ordered double perovskite $\text{PrBaCo}_2\text{O}_{5+x}$. The systems were chosen as representative of mixed conductors containing different transition metal cations and with different defect structures. The structures are illustrated in Figure 7. In perovskite, the predominant defects are oxygen vacancies whereas in La_2NiO_4 they are oxygen interstitials. Oxygen vacancies are also present in $\text{PrBaCo}_2\text{O}_{5+x}$ but are ordered in two dimensions.

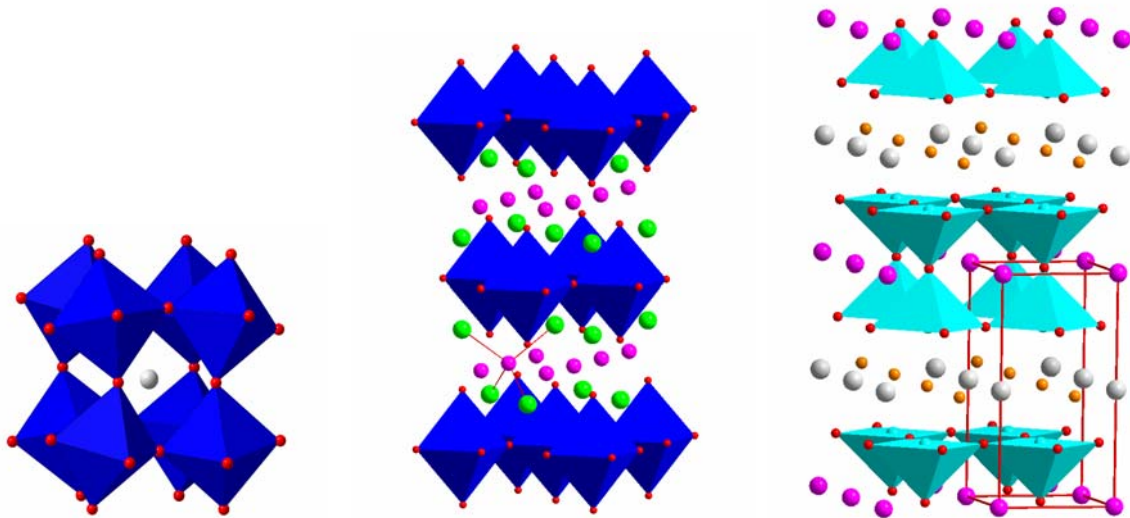


Figure 7. The structures of $\text{La}_{0.7}\text{Sr}_{0.3}\text{Cu}_{0.2}\text{Fe}_{0.8}\text{O}_{3-\delta}$, $\text{La}_2\text{NiO}_{4+x}$ and $\text{PrBaCo}_2\text{O}_{5+x}$

Samples of each of the three materials were prepared as follows:

The lanthanum strontium copper iron oxide ($\text{La}_{0.7}\text{Sr}_{0.3}\text{Cu}_{0.2}\text{Fe}_{0.8}\text{O}_{3-\delta}$) was prepared by conventional solid-state synthesis. The powder was preheated at 1050 °C for 24 h in air with a 3 °C/min of ramp rate. The preheated powder was ground with acetone in a mortar for more than 30 minutes. After drying to remove the acetone, the powder was pressed into a cylindrical shape at 15,000 psi with 1/2-inch diameter die. Dense ceramic disks were obtained by sintering in air at 1150 °C for 24 h (two times).

$\text{La}_2\text{NiO}_{4+x}$ powder was synthesized via a citrate precursor method. First, stoichiometric amounts of La_2O_3 (0.03 mol, Alfa 99.99+ %), preheated at 1000 °C in air to remove absorbed water and carbon dioxide, and NiO (0.03 mol, Aldrich, 99.99 %), preheated at 600 °C in air, were dissolved in 3M nitric acid. Ethylene glycol (13 ml, EM science, >98 %) and citric acid (17 g, Aldrich, 99.5 %) were then added to the solution. The solution was stirred at 150 °C until it foamed and eventually formed a dry resin. Further heating at 300 °C and then at 600 °C for 24 h decomposed the dry resin.

$\text{PrBaCo}_2\text{O}_{5+x}$ was also synthesized *via* a citrate precursor method. Stoichiometric amounts of Pr_6O_{11} (Alfa 99.99 %) and barium and cobalt nitrates (Aldrich, 99.99 %), were dissolved in dilute nitric acid. Ethylene glycol (EM science, >98 %) and citric acid (Aldrich, 99.5 %) were added to the solution. This mixture was covered and stirred at 150 °C until the solution began to foam and formed a dry resin. Calcination for 24 h each at 300 °C and then 600 °C decomposed the remaining organic components in the foam. The final mixture was pressed into pellets in a 1-inch diameter die followed by cold isostatic pressing (CIP). The pellet was sintered in air at 1100 °C for 12 h and then cooled down slowly (1 K min^{-1})

The phase purity of each sample was confirmed by X-ray powder diffraction. YSZ and GDC powders obtained from Tosoh and Rhodia, respectively, were used for the reactivity studies.

The table below shows the status of the experiments

| Compound | YSZ | GDC |
|--|-----|-----|
| $\text{La}_{0.7}\text{Sr}_{0.3}\text{Cu}_{0.2}\text{Fe}_{0.8}\text{O}_{3-x}$ | √ | × |
| $\text{La}_2\text{NiO}_{4+x}$ | √ | √ |
| $\text{PrBaCo}_2\text{O}_{5+x}$ | × | √ |

RESULTS AND DISCUSSION

Phase Compatibility

Two representative reactions are shown to indicate the types of experiments and the range of behavior observed.

$\text{La}_{0.7}\text{Sr}_{0.3}\text{Cu}_{0.2}\text{Fe}_{0.8}\text{O}_{3-x}$ – 8-YSZ reaction: The interaction between $\text{La}_{0.7}\text{Sr}_{0.3}\text{Cu}_{0.2}\text{Fe}_{0.8}\text{O}_{3-\delta}$ and YSZ was determined in the following manner. Figure 8a shows X-ray diffraction patterns of the reaction for 50/50 wt. % mixtures of LSCuFO7328 (1150 °C/48h) and 8-YSZ (1400 °C/4h). Heat treatments for LSCuFO-YSZ mixture were added in the temperature range 850 – 1000 °C for 2h. Weak peaks appear at $2\theta \sim 26.8, 28.1,$ and 30.7 on firing at 850 °C/2h. The intensity of these trace peaks increased as the reaction temperature increased to 950 °C especially $2\theta \sim 30.7$. Moreover, additional peaks were detected at $2\theta \sim 26.9, 31.2, 44.5,$ and 55.4 from the reaction temperature at 1000 °C. The peaks of LaSrFeO_4 ($2\theta \sim 28.1, 31.2$) are distinct from those of SrZrO_3 in the high temperature reaction. The lattice parameter changes of YSZ and LSCuFO7328 are shown in the magnified X-ray diffraction patterns in Fig. 8b. For clarity, results from the 850 and 950 °C reaction temperatures have been omitted. Note that after reaction with 8-YSZ at 1000 °C there was no apparent unit cell expansion of the YSZ whereas the sample peaks are slightly shifted to low angle side as temperature increases. Similar observations were reported by the reaction between $\text{La}_{0.8}\text{Sr}_{0.2}\text{FeO}_{3-\delta}$ and 8-YSZ [viii].

$\text{PrBaCo}_2\text{O}_{5+x}$ – CeO_2 In this case, the metal (Pr, Ba, Ce, Co) nitrates were dissolved in water and then citric acid and ethylene glycol were added to the solution. The solution was heated up until foam was formed. The foam was crushed and ground into powder and heated at 300 and then 600°C, at each temperature for 15h. Then the

powder was calcined at 1100°C for 15 h. The X-ray diffraction patterns of the product are shown in Figure 9. The diffraction data show no evidence for any reaction. As expected from the above rather severe test, no reaction was observed on firing mixtures of $\text{PrBaCo}_2\text{O}_{5+x}$ and GDC.

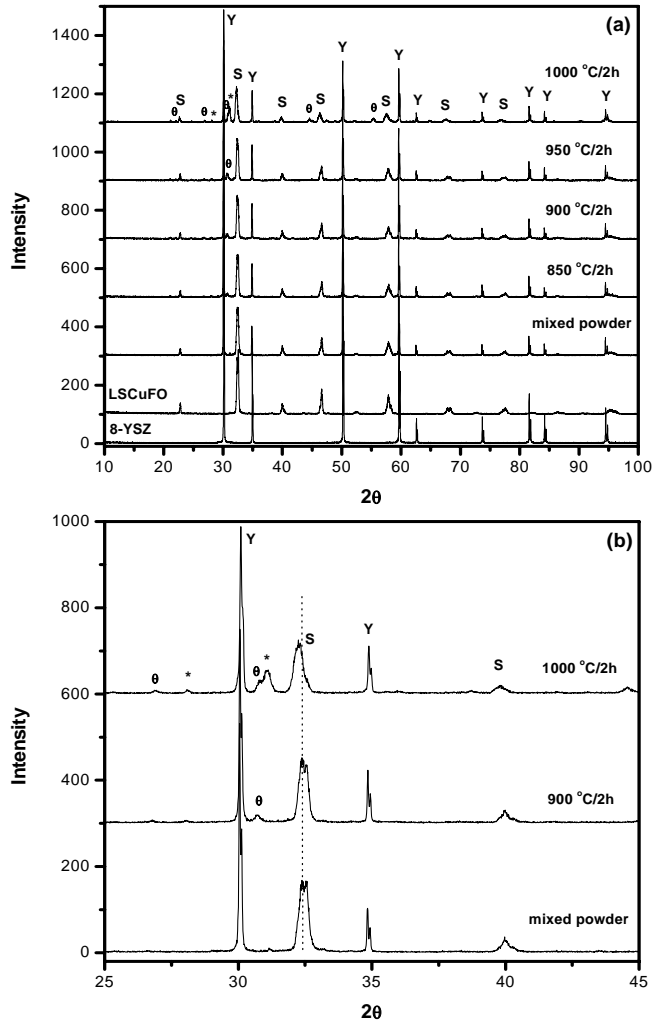


Figure 8. X-ray diffraction patterns of the reaction for (a) 50/50 wt. % 8-YSZ/ $\text{La}_{0.7}\text{Sr}_{0.3}\text{Cu}_{0.2}\text{Fe}_{0.8}\text{O}_{3-\delta}$ at $850 \leq T \leq 1000$ °C (b) magnified XRD at $25 \leq 2\theta \leq 45^\circ$. Symbols; Y: YSZ, S: Sample,

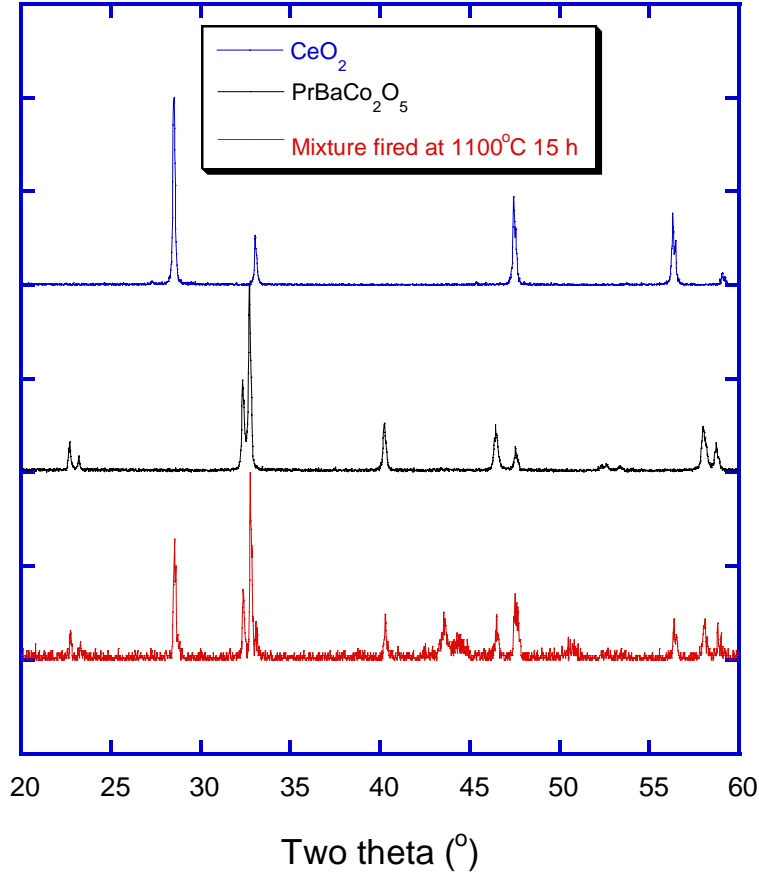


Figure 9. X-ray data showing the absence of reaction between $\text{PrBaCo}_2\text{O}_5$ and CeO_2 .

Experiments carried out by mixing powders of La_2NiO_4 and YSZ or CGO gave similar results, namely significant reaction with YSZ and little or no reaction with CGO. Based on the above results we will continue to investigate dual phase composite materials based on $\text{PrBaCo}_2\text{O}_5$ and La_2NiO_4 with CGO and CeO_2 .

Thermal expansion measurements

An important issue in the development of dual phase membranes is the relative thermal and chemical expansions of the two components. As a preliminary to permeation experiments we have measured the thermal expansion coefficient of $\text{PrBaCo}_2\text{O}_5$ and its neodymium analog. The results are shown in Figure 10. As is typical for cobalt containing systems, both the thermal and chemical expansion are large ranging from 17 to $23 \times 10^{-6} / \text{K}$ for $\text{PrBaCo}_2\text{O}_5$ and from 15 to $17 \times 10^{-6} / \text{K}$ for $\text{NdBaCo}_2\text{O}_5$. In contrast

previous measurements give a much smaller value of $13.7 \times 10^{-6} /\text{K}$ for La_2NiO_4 which is close to the value for CGO of $13.5 \times 10^{-6} /\text{K}$.

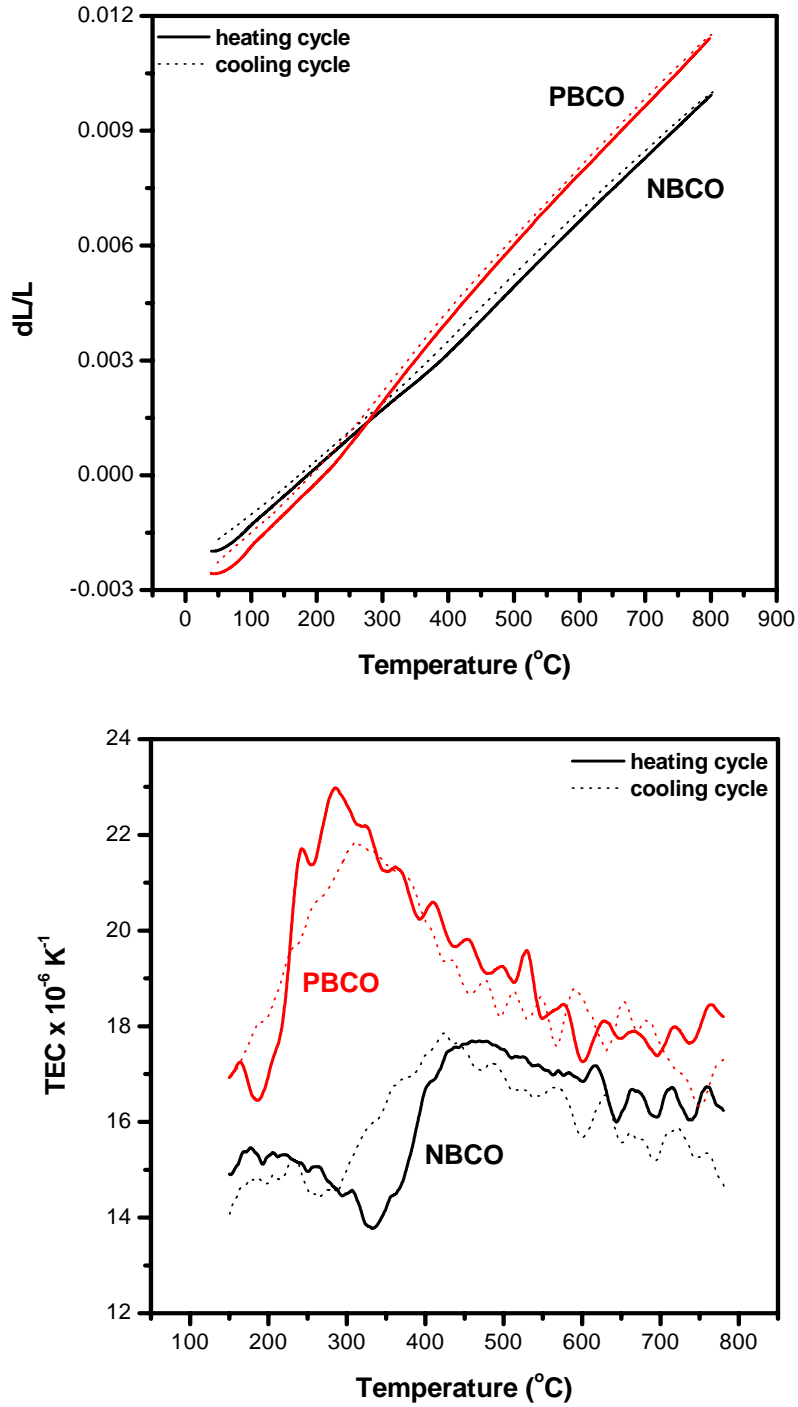


Figure 10 Thermal and chemical expansion of $\text{PrBaCo}_2\text{O}_5$ (PBCO) and $\text{NdBaCo}_2\text{O}_5$ (NBCO).

Plans for the Next Quarter.

In the next quarter we will carry out densification studies of both La_2NiO_4 and $\text{PrBaCo}_2\text{O}_5$ composites with CGO and CeO_2 . The initial compositions will use 25 and 50 % CGO to cover the range above and below the CGO percolation threshold. We will measure the thermal expansion coefficients of the composite materials. Assuming that dense samples can be prepared, we will then carry out permeation measurements. A new apparatus for this purpose has been constructed and tested during the last quarter.

CONCLUSIONS

The total weight loss in the N₂ atmosphere is significantly higher than the weight loss obtained in air. Also, the weight loss is completely irreversible in N₂ atmosphere. Overall, in the case of N₂ atmosphere, the decomposition of membranes has started earlier than in air.

Thermal strength at room temperature and at 1000°C in N₂ atmosphere was carried out for LSFT-CGO membrane. The flexural strength value obtained for dual phase membrane (LSFT-CGO) at room temperature and at 1000°C in N₂ is 245 and 107.5MPa respectively.

We have demonstrated that PrBaCo₂O₅ and La₂NiO₄ are both compatible with CGO and we will we pursue investigations of dual phase composite membranes base on these systems. Densification studies are in progress and will be followed by thermal expansion and permeation measurements.

LIST OF ACRONYMS AND ABBREVIATIONS

| | |
|-----|---------------------------|
| CGO | Cerium gadolinium oxide |
| GDC | Gadolinia doped ceria |
| YSZ | Ytria stabilized zirconia |
| XRD | X-ray diffraction |

REFERENCES

Task 2

1. Zhou *et al*, OTM annual report 2005, page 10

Task 3

- [i] H. J. M. Bouwmeester, A. J. Burggraaf, “*The CRC Handbook of Solid State Electrochemistry*”, Eds. P. J. Gellings and H. J. M. Bouwmeester, CRC Press, Boca Raton, (1997) 481.
- [ii] J. Yoo, A. Verma, and A. J. Jacobson, Proc. Electrochem. Soc. PV2001-28 (2002) 27.
- [iii] J. Yoo, A. Verma, S. Wang, and A. J. Jacobson, J. Electrochem. Soc. 152 (2005) A497.
- [iv] C. Y. Park and A. J. Jacobson, J. Electrochem. Soc. 152 (2005) J65.
- [v] C. Y. Park and A. J. Jacobson, Solid State Ionics 176/35-36 (2005) 2671.
- [vi] J. Yoo, C. Y. Park and A. J. Jacobson, Solid State Ionics 175(1-4) (2004) 55.
- [vii] T. H. Lee, Y. L. Yang, A. J. Jacobson, Solid State Ionics, 134 (2000), 331 and references therein.
- [viii] S. P. Simner, J. P. Shelton, M. D. Anderson, and J. Stevenson, Solid State Ionics, **161** (2003) 11.